Journal of
Computational and Theoretical Nanoscience
Vol. 7, 1–14, 2010

Elastic Properties and Frequencies of Free Vibrations of Single-Layer Graphene Sheets

S. S. Gupta and R. C. Batra*

Department of Engineering Science and Mechanics, M/C 0219 Virginia Polytechnic Institute and State University Blacksburg, VA 24061, USA

We determine the basal plane stiffness and Poisson's ratio of single layer graphene sheets (SLGSs) in armchair and zigzag directions by using molecular mechanics simulations of their uniaxial tensile deformations with the MM3 potential, and of their axial and bending vibrations. Both approaches give the basal plane stiffness equal to ∼340 N/m which agrees well with that reported in the literature and derived from results of indentation experiments on SLGSs and from the first principle calculations. The computed value of Poisson's ratio equals 0.21 in both armchair and zigzag directions. Assuming that the response of a SLGS is the same as that of a plate made of a linear elastic, homogeneous, and isotropic material having Poisson's ratio = 0.21, the in-plane stiffness of ∼340 N/m and the total mass equal to that of the SLGS, the thickness of the SLGS is found to be ∼1 Å. Thus Young's modulus and the shear modulus of a SLGS equal ∼3.4 TPa and ∼1.4 TPa, respectively. It is shown that mode shapes corresponding to the several lowest frequencies of the SLGS differ noticeably from those of an equivalent thin layer made of a linear elastic isotropic material with Young's modulus = 3.4 TPa and the shear modulus = 1.4 TPa. Furthermore, a free–free SLGS vibrates about a plane bisecting its width rather than its thickness as predicted by the Euler Bernoulli beam theory. We also investigate the effect of pretension on the natural frequencies of SLGSs using MM simulations and correlate it to that of 1 Å thick linear elastic plate found by analyzing its three-dimensional deformations. These results will help design SLGS nanomechanical resonators having frequencies in the THz range.

Keywords: Single Layer Graphene Sheet, Frequencies, Thickness, Elastic Constants.

RESEARCH ARTICLE

1. INTRODUCTION

An atom thick graphene sheet comprised of a hexagonal network of covalently bonded carbon atoms is expected to exhibit novel mechanical and electronic properties. These sheets may be used as reinforcements in composite materials to acquire high specific strength or as nanomechanical resonators in THz frequency range. Since the discovery of carbon nanotubes by Iijima[1] in an arc discharge evaporation experiment, it has been anticipated that these tubes could be engineered economically if it were possible to control the geometry of graphene sheets. Hiura et al.[2] used an atomic force microscope (AFM) tip to cleave highly oriented pyrolytic graphite (HOPG) and imaged two single layer graphene sheets (SLGSs) separated by 3.4 Å. They also imaged folding and unfolding of graphitic layers, and observed that tearing and folding of graphitic layers was governed by the formation of sp^3 like line defects in the sp^2 graphitic networks. Similarly Roy et al.[3] studied the cleaved HOPG and performed folding and unfolding of atomic layers of graphite using scanning tunneling microscope (STM). They found that the tip vibration of the STM can tear the graphitic layers. Lu et al.[4] patterned the HOPG surface with oxygen plasma etching to create uniformly sized islands up to 9 μm in size and peeled graphene sheets from these islands for further manipulation with AFM tips. Recently Novoselov et al.[5] have prepared SLGSs using micromechanical cleavage. Stankovich et al.[6] have developed a technique to fabricate graphene-polymer composites via complete exfoliation of graphite and molecular-level dispersion of individual, chemically modified graphene sheets in the host polymer. We review below the pertinent literature on the modeling of graphene sheets through experimental, analytical and numerical approaches.

The structural applications of graphene require that we know its macroscopic properties. Previous theoretical and experimental studies have used continuum theories to determine basal plane stiffness ($K = Eh$, E: Young's modulus, h: wall thickness shown in Fig. 1), Poisson's ratio

*Author to whom correspondence should be addressed.

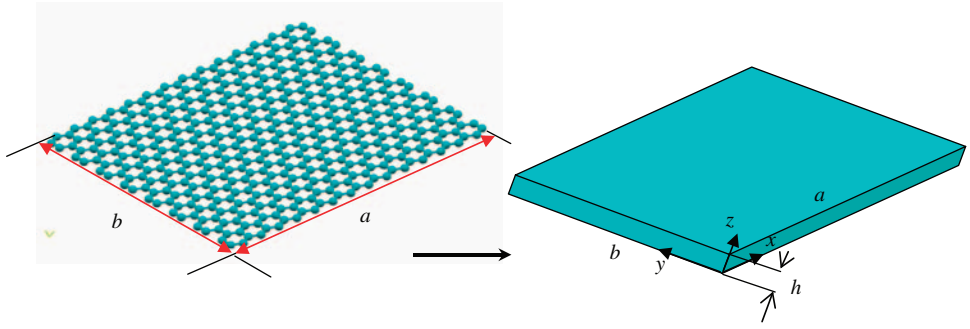

Fig. 1. Thin plate equivalent in mechanical response to a SLGS.

ν, and bending stiffness $D = Eh^3/12(1\text{-}\nu^2)$ of a SLGS by representing it as a homogeneous, linear elastic, and transversely isotropic plate[7] with the axis of transverse isotropy perpendicular to the basal plane. A SLGS is an atom thick. In order to determine its equivalent continuum structure (ECS) shown in Figure 1, some researchers have either computed the wall thickness h or have assumed it to be 3.4 Å which is the interlayer separation in bulk graphite. Table I summarizes values of K, V, h and D reported in the literature using different theoretical and experimental methods.

Behfar and Naghdabadi[25] used the classical plate theory (CPT) to study vibrations of simply supported two-layered graphene sheets embedded in an elastic medium, and assumed them to be orthotropic in their planes with Young's moduli E_1 and E_2 in the two principal directions as 1765 GPa and 1588 GPa, respectively, the in-plane Poisson's ratio ν_{12} as 0.3, the thickness of a SLGS = 3.4 Å,

Table I. Values of K, h, D and n computed from atomistic simulations and experiment reported in the literature.

Author(s)	Year	Potential/Method	K (Nm^{-1})	ν	h (Å)	D (eV)
Van Lier et al. [8]	2000	*Ab initio*	~377	—	3.4	—
Kudin et al. [9]	2001	*Ab initio*	345	0.149	0.894	1.5
Aroyo and Belytschko [10]	2004	Brenner				
		First generation	236	0.412	—	0.846
		Second generation	243	0.397		0.690
Huang et al. [11]	2006	Brenner (First generation)				
		—Uni-axial tension	~235	0.412	0.618	0.562[a]
		—Uni-axial stretching	~236	0.412	0.734	0.797[a]
		—Equi-biaxial stretching	~235	0.412	0.874	1.125[a]
		Brenner (Second generation)				
		—Uni-axial tension	~243	0.397	0.574	0.494[a]
		—Uni-axial stretching	~243	0.397	0.678	0.690[a]
		—Equi-biaxial stretching	~242	0.397	0.811	0.983[a]
Reddy et al. [12]	2006	Tersoff-Brenner				
		Along zigzag edge (direction -1)	~227	$\nu_{12} = 0.416$	3.4	
		Among armchair edge (direction -2)	~276	$\nu_{21} = 0.465$		—
Konstantinova et al. [13]	2006	Density Functional Theory	~420	—	—	—
Liu et al. [14]	2007	*Ab initio*	~357	0.186	3.4	—
Lee et al. [15]	2008	Nano-indentation (Experimental)	340 ± 50	—	—	—
Michel and Verberck [16]	2008	Harmonic lattice dynamics theory	~ 385	0.228	—	1.12
Zhou and Huang [17]	2008	Tersoff-Brenner				
		Without internal lattice relaxation	~339	0.158	—	
		With internal lattice relaxation	~236	0.414		—
Faccio et al. [18]	2009	Density functional theory	323	0.18	—	—
Sakhaee-Pour [19]	2009	Atomistic structural mechanics	~354	>1.0	3.4	—
Bu et al. [20]	2009	Tersoff-Brenner	~415	—	3.35	—
Scarpa et al. [21]	2009	Atomistic structural mechanics				
		AMBER and morse	64–546	0.21–0.85	0.74–0.99	—
Lu et al. [22]	2009	Empirical potential	—	—	—	1.4
Klintenberg et al. [23]	2009	Density Functional Theory	358	—	—	—
Cadelano et al. [24]	2009	Tight-binding atomistic simulations	312	0.31	—	—

[a]Computed from values of E, h and ν provided by the author(s).

and the mass density = 2300 kg/m^3. They modeled the interlayer interaction and the interaction between the outer layers and the matrix with van der Waals forces. They found that there are two frequencies for the same pair of half wave numbers along the length and the width directions. The mode corresponding to the lower of these two frequencies has both sheets moving in phase whereas that corresponding to the higher frequency has both sheets moving in opposite directions. Furthermore, an increase in the stiffness between the outer graphene layers and the polymer matrix enhanced the two frequencies. He et al.[26] used the CPT to study the effect of interlayer van der Waals forces on resonant frequencies of simply supported multilayer graphene sheets (MLGSs). The interlayer distance, Young's modulus, and the mass density are taken as 3.4 Å, 1.02 TPa and 2250 kg/m^3, respectively. They found that the number of solutions for the natural frequencies equaled the number of layers. The smallest natural frequency corresponding to a pair of half wave numbers along the length and the width directions was found to be independent of the interlayer van der Waals force parameter. Liew et al.[27] analysis is similar to that of Behfar and Naghdabadi[25] except that the interaction of the outer graphene sheets with polymeric matrix is modeled using Pasternak foundation which accounts for the shear and the normal deformations of the surrounding elastic medium. They concluded that the elastic medium has a little effect on the amplitudes of vibrations of the sheets but no effect on the resonant frequencies. Bunch et al.[28] fabricated and tested SLGSs and MLGSs based electromechanical resonators by suspending a micrometer long graphene sheet over SiO_2 trench. The clamping of the opposite edges of the graphene sheet on the SiO_2 trench was due to van der Waals forces. They experimentally determined frequencies of SLGSs by actuating them either electrically or optically, and modeled them as a clamped–clamped Euler Bernoulli beam with uniform initial tension, assumed its thickness to be 3 Å, the mass density = 2200 kg/m^3, and $E = 1.0$ TPa.

Using the MM3 potential, we simulate in-plane tensile deformations of graphene strips to determine their basal plane stiffness and Poisson's ratio in zigzag and armchair configurations. This value of the basal plane stiffness is compared with that obtained by studying free axial and bending vibrations of a SLGS traction free on all four edges. The thickness of a SLGS is determined by modeling it as a plate made of a linear elastic, homogeneous and isotropic material and equating frequencies of the plate to those of the SLGS and same boundary conditions applied to the plate and the SLGS; we call the plate an equivalent continuum structure (ECS). An ECS of a SLGS enables one to use homogenization techniques for determining elastic properties of polymeric composites with SLGSs used as reinforcements. Furthermore, these ECSs can be used to compute first few natural frequencies of nanomechanical resonators, and find their optimum geometric parameters. The frequency of the fundamental mode of vibration of a SLGS can be increased to a THz by inducing in-plane tension in them; we study this by using MM simulations for a SLGS and the three-dimensional linear elasticity theory for its ECS.

The rest of the paper is organized as follows. Section 2 describes the MM3[29] potential and Section 3 details of our MM simulations of the uniaxial tensile deformations of a SLGS, computation of the basal plane stiffness and Poisson's ratio. The basal plane stiffness found from frequencies of the axial and the bending modes of vibration are described in Section 4. In Section 5 we determine the thickness of the ECS of a SLGS based on the basal plane stiffness and Poisson's ratio found in Section 3. It is shown in Section 6 that various modes of vibration of a free SLGS computed via MM simulations do not agree with those of its ECS found using the three-dimensional linear elasticity theory. In Section 7 we investigate effects of pretension on natural frequencies of SLGSs. Conclusions drawn from this work are summarized in Section 8.

2. MOLECULAR MECHANICS POTENTIAL

The MM3[29] class II potential with both higher-order expansions and cross-terms is appropriate for modeling SLGSs due to the similarity between graphitic bonds in the SLGSs and the aromatic protein structures for which the potential was constructed. The potential is given by Eq. (1) in which U_s, U_θ and U_ϕ are energies due to bond stretching, bending and torsion respectively; U_{vdW} is the potential of non-bonded van der Waals forces, and $U_{s\theta}$, $U_{\phi s}$ and $U_{\theta\theta'}$ represent energies of cross interactions between stretch-bend, torsion-stretch and bend–bend deformations, respectively. Parameters r, θ, θ' and ϕ in Eq. (1) are shown in Figure 2. A subscript, e, on a variable signifies its value in the configuration of the minimum potential energy. The total potential energy of a body equals the sum of potential energies of all atoms in the body (indices i and j in Eq. (1) range over bonded atoms, and the index k over all atoms).

$$U = \sum_i \sum_j (U_s + U_\theta + U_\phi + U_{s\theta} + U_{\phi s} + U_{\theta\theta'}) + \sum_i \sum_k U_{vdW}$$

$$U_s = 71.94 K_s (r - r_e)^2 \left[1 - 2.55(r - r_e) + \left(\frac{7}{12}\right) 2.55 (r - r_e)^2 \right]$$

$$U_\theta = 0.021914 K_\theta (\theta - \theta_e)^2 [1 - 0.014(\theta - \theta_e) + 5.6(10)^{-5}(\theta - \theta_e)^2 - 7.0(10)^{-7}(\theta - \theta_e)^3 + 9.0(10)^{-10}(\theta - \theta_e)^4]$$

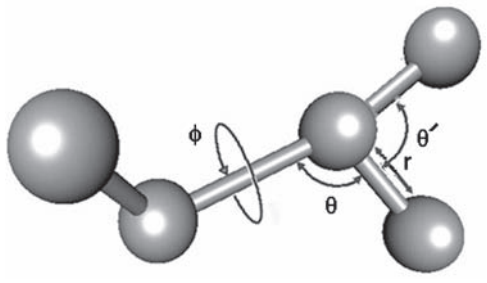

Fig. 2. Depictions of variables r, θ, θ' and ϕ used in the expression for the MM3 potential.

$$
\begin{aligned}
U_\phi &= (V_1/2)(1+\cos\phi)+(V_2/2)(1-\cos 2\phi)\\
&\quad +(V_3/2)(1+\cos 3\phi)\\
U_{s\theta} &= 2.51118K_{s\theta}[(r-r_e)+(r'-r_e')](\theta-\theta_e)\\
U_{\phi s} &= 11.995(K_{\phi s}/2)(r-r_e)(1+\cos 3\phi)\\
U_{\theta\theta'} &= -0.021914K_{\theta\theta'}(\theta-\theta_e)(\theta'-\theta_e'), \quad \text{and}\\
U_{vdW} &= \varepsilon_e\{-2.25(r_v/r)^6+1.84(10)^5\exp[-12.0(r/r_v)]\}
\end{aligned}
\tag{1}
$$

Values of constants K_s, K_θ, V_1, V_2, V_3, ε_e, r_v, $K_{s\theta}$, $K_{\phi s}$ and $K_{\theta\theta'}$ are given in Ref. [29]. Note that the van der Waals force between two atoms varies as $(r_v/r)^6$ and $\exp(-12r/r_v)$. The first term is the same as that in the Lennard-Jones potential, but the second term is different. Because of the term $(r-r_e)^3$ in the expression for U_s, the potential energy for tensile and compressive deformations involving equal changes in bond lengths are different.

As listed in Table III of Gupta and Batra[30] the MM3 potential used herein gives frequencies of radial breathing modes of SWCNTs which agree well with their experimental values. Since no structural model is used in this comparison, the close agreement between the computed and the experimental values provides one measure of the validity of the MM3 potential to model SWCNTs. Also, except for the Coulomb force due to point charges, expressions in the MM3 potential are essentially the same as those in the Condensed-phase Optimized Molecular Potentials for Atomistic Simulation Studies (COMPASS) often used to simulate deformations of polymeric materials.[31] Another indication of the suitability of the MM3 potential for SWCNTs is that the computed basal plane stiffness of 340 N/m is very close to experimental mean value of 340 N/m found by Lee et al.[15]

3. MM SIMULATIONS OF UNIAXIAL TENSILE DEFORMATIONS

Uniaxial tensile deformations of graphene strips of aspect ratio ~10 are conducted using the MINIMIZATION module of the software TINKER[32] by constraining displacements of all atoms at one end in x, y and z—directions and prescribing incremental displacements of all atoms at the other end along the length direction and constraining them to their new positions in x, y and z—directions. Two configurations, namely armchair and zigzag, depicted in Figure 3 of graphene strips are considered. For an armchair strip atoms on the edge 1L are constrained while atoms on the edge 1R have prescribed x-displacement; for a zigzag strip atoms on the edge 2B are constrained while atoms on the edge 2T have prescribed y-displacement.

After every incremental prescribed displacement the minimum potential energy configuration of a SLGS is obtained to within rms potential gradient of 0.001 kcal/mol/Å without using any cut-off distance. From the gradient of the potential energy of each atom for which the displacement is prescribed, forces acting on that atom are computed. Force per unit length (N_x and N_y for armchair and zigzag strips, respectively) are determined by dividing the total force acting on atoms on the edge by the length of the edge. Components of the strain tensor in the strip are computed from the mean-value of the deformation gradient[33] using three nearest atoms surrounding the one of interest. For both armchair and zigzag SLGSs the strain field is found to be uniform except at atoms near the edges where displacements are prescribed.

For a 262.24 Å × 23.53 Å armchair SLGS, we have plotted in Figure 4 components of the strain tensor when atoms on the edge 1R of the strip are displaced by 1 Å in the x-direction while keeping atoms on the edge 1L fixed. The strain component E_{yy} is negative due to Poisson's effect, and the shear strain E_{xy} equals zero indicating that most of the SLGS is deformed in simple tension. The relation between N_x and E_{xx} for atoms at the sheet centroidal axis parallel to the loaded edge is shown in Figure 5. The straight line fitted through the data by the least-squares method has a slope of 486.7 kcal/mole/Å^2 or 338.11 N/m; this equals the basal plane stiffness.

For a 22.76 Å × 260.06 Å zigzag graphene strip we have displayed in Figure 6 components of the strain tensor

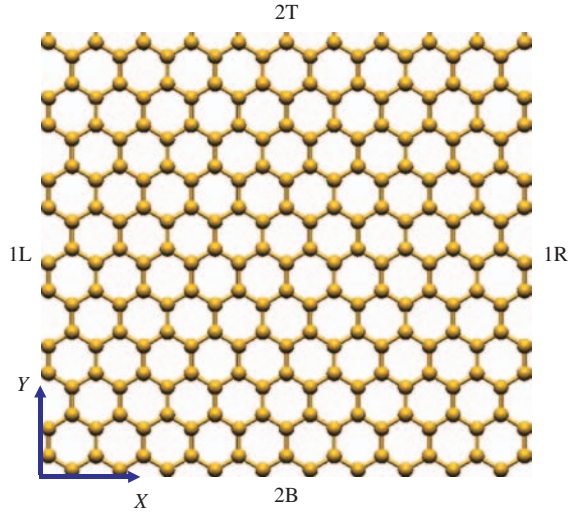

Fig. 3. Segment of a graphene strip with armchair (1L, 1R) and zigzag (2T, 2B) edges.

RESEARCH ARTICLE

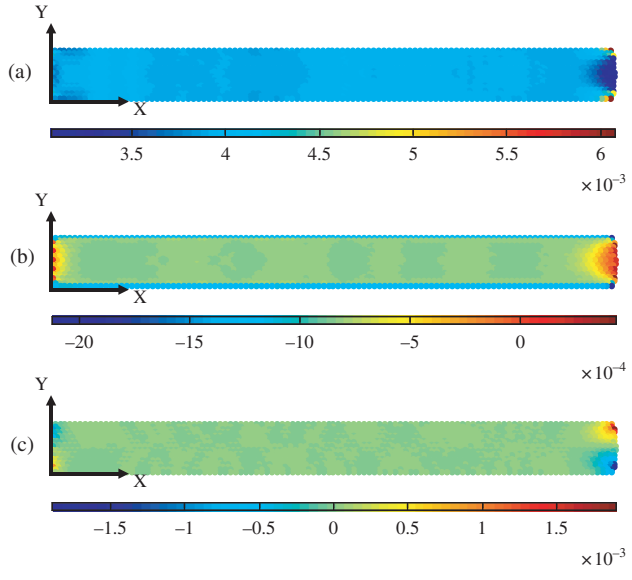

Fig. 4. Distribution of strains in the 262.24 Å × 23.53 Å armchair graphene strip for 1 Å x-displacement of atoms on the right edge with atoms on the left edge kept fixed; (a) E_{xx}, (b) E_{yy}, and (c) E_{xy}.

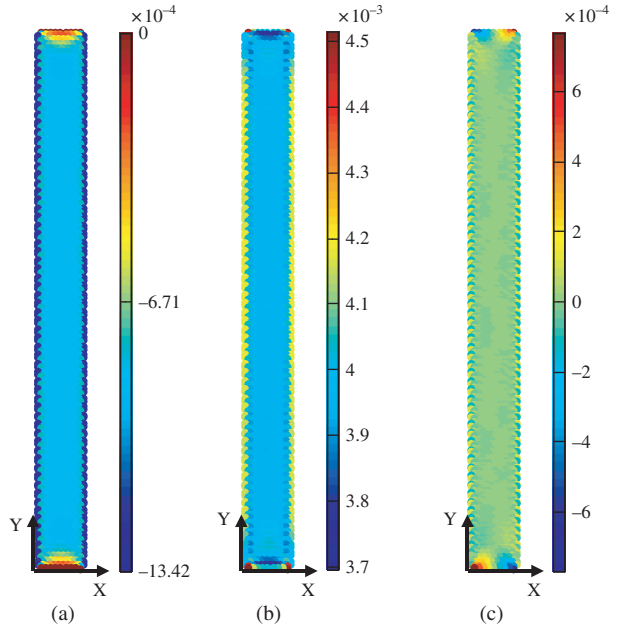

Fig. 6. Distribution of strains in the 22.76 Å × 260.06 Å zigzag graphene strip for 1 Å x-displacement of atoms on the right edge with atoms on the left edge kept fixed; (a) E_{xx}, (b) E_{yy}, and (c) E_{xy}.

when atoms on the edge 2T of the strip are displaced by 1 Å in the y-direction while atoms on the edge 2B are fixed. For this case the strain component E_{xx} is negative due to Poisson's effect, and as in the previous case, the shear strain E_{xy} is zero. The slope of the straight line fitted through (N_y, E_{yy}) by the least squares method equals 489.54 kcal/mole/Å^2, or 340.08 N/m; this equals the basal plane stiffness.

3.1. Determination of Poisson's Ratio in the Basal Plane

From average values of the axial and the lateral strains for the two SLGSs studied above, the Poisson ratio is found to be 0.21. Since $K_x = K_y$ and $\nu_{xy} = \nu_{yx}$, we conclude the following: it is reasonable to assume that mechanical deformations of a SLGS are equivalent to those of an ECS that is isotropic in the plane of the sheet. Thus material of the ECS and hence the SLGS can be regarded as transversely isotropic with the axis of transverse isotropy perpendicular to the plane of the ECS or the SLGS having the basal plane stiffness $K =\sim 340$ N/m and Poisson's ratio $=\sim 0.21$. These values agree well with the experimental and numerical values from *ab initio* computations listed in Table I.

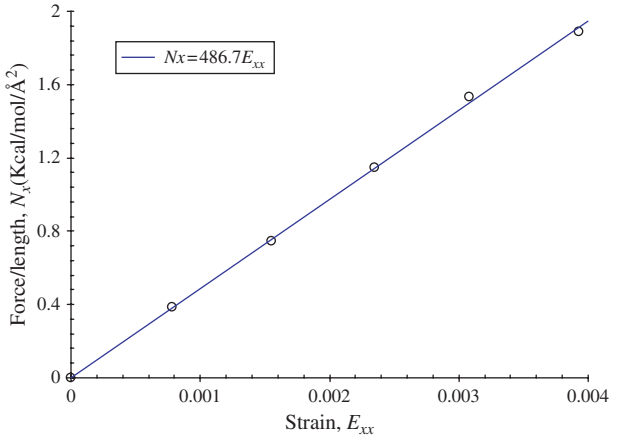

Fig. 5. N_x versus E_{xx} for the 262.24 Å × 23.53 Å armchair graphene strip.

4. EVALUATION OF BASAL PLANE STIFFNESS FROM FREE VIBRATIONS OF SLGSs

As for the static axial deformations the SLGSs of aspect ratio ∼10 are first relaxed to find the minimum energy configuration to within 0.001 kcal/mol/Å rms without using any cut-off distance. The aspect ratio of ∼10 of the SLGS and hence of its ECS minimizes transverse inertia effects thus enabling us to use the 1-D wave equation to study axial vibrations, and the Euler-Bernoulli beam theory (EBBT) to study the fundamental mode of bending vibrations. The module VIBRATE in computer code TINKER[32] is used to calculate eigenvalues and eigenvectors of the mass weighted Hessian matrix of the equilibrated SLGSs with all edges kept free of any applied load. The eigenvector associated with an eigenvalue is used to identify the corresponding mode of vibration; these are compared with the natural frequencies of the ECS for the same mode of vibration by assuming the material of the ECS to be linear elastic, homogeneous and isotropic. We

RESEARCH ARTICLE

Table 2A. Frequencies of axial and bending modes of vibrations of a free–free SLGS of aspect ratio 10, and values of the basal plane stiffness computed from these frequencies.

Graphene strip (Size) (C-atoms)	Mode No.	ω^{A} (cm^{-1})	ω^{B} (cm^{-1})	$(Eh)_{Axial}$ (N/m)	$(Eh)_{Bending}$ (N/m)
Armchair	1	12.741	2.364	344.1	348.0
(23.53 Å × 262.24 Å)	2	25.467	6.220	343.7	317.2
(2652)	3	38.162	11.467	343.0	280.5
Zigzag	1	12.656	2.321	347.4	360.9
(22.76 Å × 260.06 Å)	2	25.303	6.098	347.1	327.8
(2652)	3	37.923	11.247	346.5	290.2
Armchair	1	8.628	1.620	339.9	331.6
(35.98 Å × 389.16 Å)	2	17.246	4.269	339.5	303.1
(5886)	3	25.843	7.861	338.8	267.4
Zigzag	1	8.560	1.673	341.3	338.4
(37.12 Å × 388.66 Å)	2	17.114	4.374	341.1	304.2
(6204)	3	25.647	8.017	340.5	265.9

have listed in Table II the first three frequencies of axial and bending modes of oscillations for two armchair and the two zigzag SLGSs of different sizes. As for frequencies of the ECS, we note that for each SLGS studied, frequencies of the 2nd and the 3rd axial modes of vibration are very close to twice and three times the corresponding frequency of the 1st mode. It is thus reasonable to assume that an ECS is a prismatic strip, and its length and breadth equal that of the relaxed graphene strip. We now postulate that the thickness, Young's modulus and the shear modulus of the ECS are such that its frequencies of free vibrations equal those of the corresponding SLGS for axial and bending modes of vibration.

Frequencies $\omega_{n\mathrm{A}}$ (rad/sec) of the nth axial mode, and $\omega_{n\mathrm{B}}$ (rad/sec) of the nth bending mode of vibration of the ECS are given by[34]

$$\omega_{n\mathrm{A}} = \frac{n\pi}{l_e}\sqrt{\frac{E}{\rho}} \quad n = 1, 2, 3, \ldots \tag{2}$$

Table 2B. Frequencies of bending modes of vibrations of a free–free SLGS of aspect ratios 15 and 20, and values of the basal plane stiffness computed from these frequencies.

Graphene strip (Size) (C-atoms)	Mode No.	ω^{B} (cm^{-1})	$(Eh)_{Bending}$ (N/m)
Armchair	1	1.285	357.787
(23.53 Å × 358.64 Å)	2	3.467	342.928
(3612)	3	6.551	318.508
Zigzag	1	1.234	344.628
(23.34 Å × 359.66 Å)	2	3.312	326.659
(3654)	3	6.262	303.778
Armchair	1	0.651	347.946
(23.35 Å × 496.59 Å)	2	1.774	340.229
(5040)	3	3.409	326.904
Zigzag	1	0.713	348.251
(23.53 Å × 478.36 Å)	2	1.984	354.882
(4812)	3	3.813	340.996

Table 3. Frequencies of various bending modes of vibrations of nearly square SLGSs and values of the thickness computed from Eq. (4).

	Size of graphene Sheet (C-atoms)	Modes $(r, s)^{a}$	Frequency (THz)	Equivalent thickness 'h' (Å)
(A)	20.31 Å×19.42 Å	(1,1)	0.677	0.82
	(180)	(1,2)	1.637	0.97
		(2,1)	1.722	1.02
		(2,2)	2.602	1.05
(B)	32.33 Å × 31.83 Å	(1,1)	0.259	0.80
	(464)	(1,2)	0.623	0.95
		(2,1)	0.656	1.00
		(2,2)	1.006	1.04
		(1,3)	1.222	1.04
(C)	67.15 Å × 66.99 Å	(1,1)	0.074	0.97
	(1881)	(1,2)	0.157	1.01
		(2,1)	0.160	1.03
		(2,2)	0.248	1.08
		(1,3)	0.307	1.10

[a] r and s are the number of half waves along the x- and the y- axes respectively.

$$\omega_{n\mathrm{B}} = \frac{\beta_n^2}{l_e^2}\sqrt{\frac{EI}{\rho A}}; \quad n = 1, 2, 3 \ldots, \tag{3}$$

where E, ρ and l_e equal, respectively, the axial Young's modulus, the mass density and the length of the ECS, and I is the second moment of area of cross section A of the ECS. The expression for frequencies in Eq. (3) assumes that the structure can be modeled as an Euler-Bernoulli beam, and for the first three bending modes $\beta_1 = 4.730$, $\beta_2 = 7.853$ and $\beta_3 = 10.996$.

Equating $\omega_{n\mathrm{A}}$ and $\omega_{n\mathrm{B}}$ to the corresponding frequencies of the SLGS found through MM simulations, we evaluate the basal plane stiffness of the ECS; these values are listed in Table II(A). We note that values of K computed from $\omega_{n\mathrm{A}}$ for the four SLGSs studied here are nearly the same, 342 ± 0.3 N/m., and agree well with that obtained from the uniaxial tensile tests on SLGSs. The experimentally determined[15] value of K is 340 ± 50 N/m. However, values of K computed from $\omega_{n\mathrm{B}}$ decrease with an increase in the mode number, n. The first bending mode frequency for the four cases gives $K = 344 \pm 12.7$ N/m, but the 2nd and the 3rd bending mode frequencies yield $K \approx 317$ and 280 N/m, respectively. This most likely is due to the inapplicability of the EBBT to a beam of aspect of aspect ratio ~10 for finding frequencies of the 2nd and the 3rd mode.

Table 4. Frequencies of the axial and the bending modes of oscillations computed from the MM simulations and the FE method with the ECS modeled as a thin shell.

Graphene strip (Size) (C-atoms)	Mode No.	MM ω^{A} (cm^{-1})	FEM ω^{A} (cm^{-1})	MM ω^{B} (cm^{-1})	FEM ω^{B} (cm^{-1})
Armchair	1	12.741	12.673	2.364	2.276
(23.53 Å × 262.24 Å)	2	25.467	25.337	6.220	5.998
(2652)	3	38.162	37.982	11.467	11.106

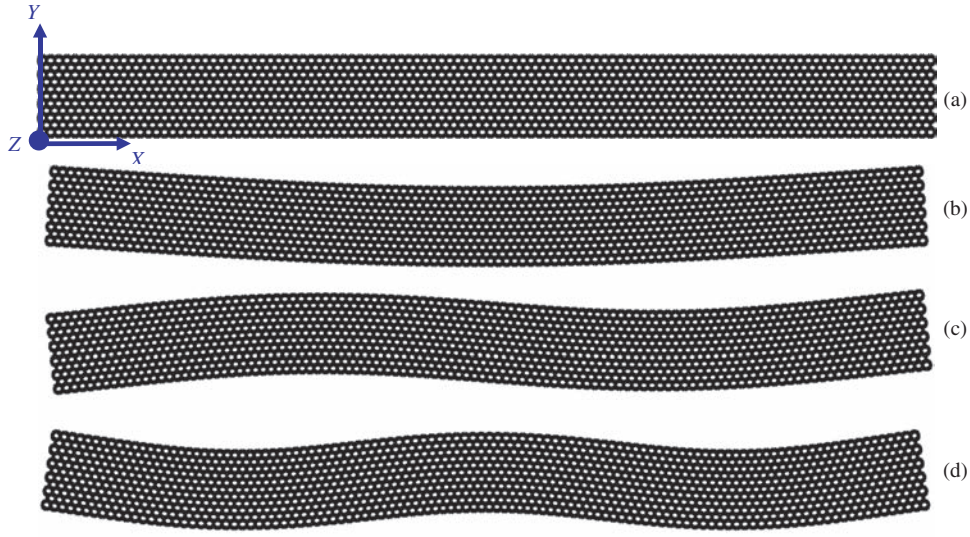

Fig. 7. Beam type bending modes of free–free 23.53 Å × 262.24 Å armchair graphene strip; (a) equilibrated structure, (b) first bending mode, (c) second bending mode, and (d) third bending mode. Bending deformations occur in the plane of the strip.

Accordingly, we studied vibrations of a free–free SLGS of aspect ratio 20, and the corresponding results listed in Table II(B) evince that indeed the aspect ratio of the sheet plays a significant role in deciding whether or not to use the EBBT for studying higher order modes of vibration of the sheet. An unanticipated result is that the free–free SLGSs vibrate about the plane bisecting the width rather than the thickness as predicted by the EBBT.

5. THICKNESS OF SLGSs FROM FREQUENCIES OF FREE VIBRATIONS

In an attempt to find the thickness of a SLGS, we study free vibrations of clamped square SLGSs of different dimensions following the procedure outlined above. The Hessian computed from the TINKER software is exported to MATLAB[35] for mass weighting, applying essential

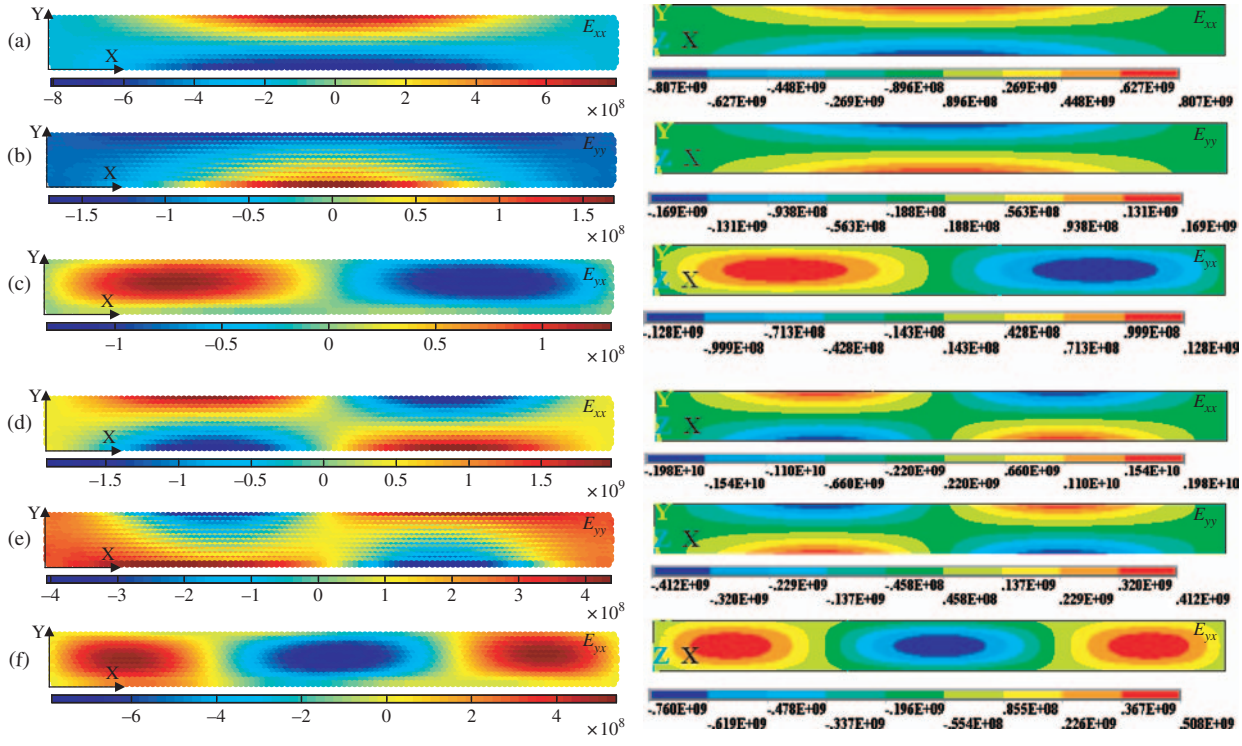

Fig. 8. Comparison of strains from the MM simulation results (left) and the analysis of the ECS (right); (a), (b) and (c) for the first bending mode and (d), (e) and (f) for the second bending mode.

boundary conditions, and computing frequencies and mode shapes.

The bending mode frequencies for various combinations of half waves along the x- and the y- axes are listed in Table III for the clamped SLGSs, and are compared with frequencies of their ECSs using the CPT. Frequencies of bending modes of vibration, f_{rs}^{P} (Hz), of thin plates ($a/h > 15$, where a and h are the length of the smallest side and the thickness, respectively) made of a linear elastic, homogeneous and isotropic material of uniform thickness are given by[34]

$$f_{rs}^{P} = \frac{\lambda_{rs}^2}{2\pi a^2}\left[\left(\frac{Eh^3}{12\gamma(1-\nu^2)}\right)\right]^{1/2}; \quad r = 1, 2, 3, \ldots \text{ and } s = 1, 2, 3, \ldots \tag{4}$$

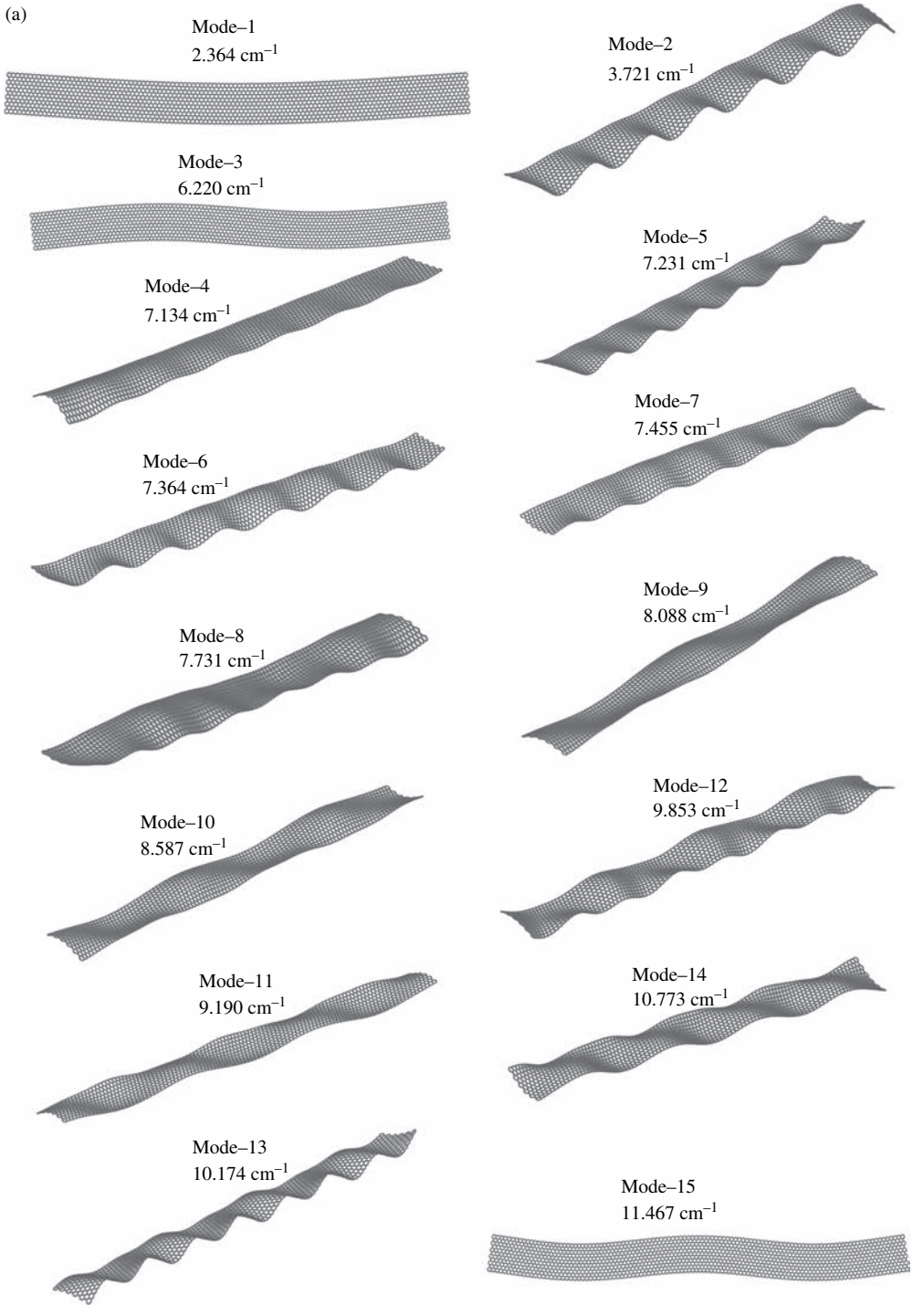

Fig. 9. Continued.

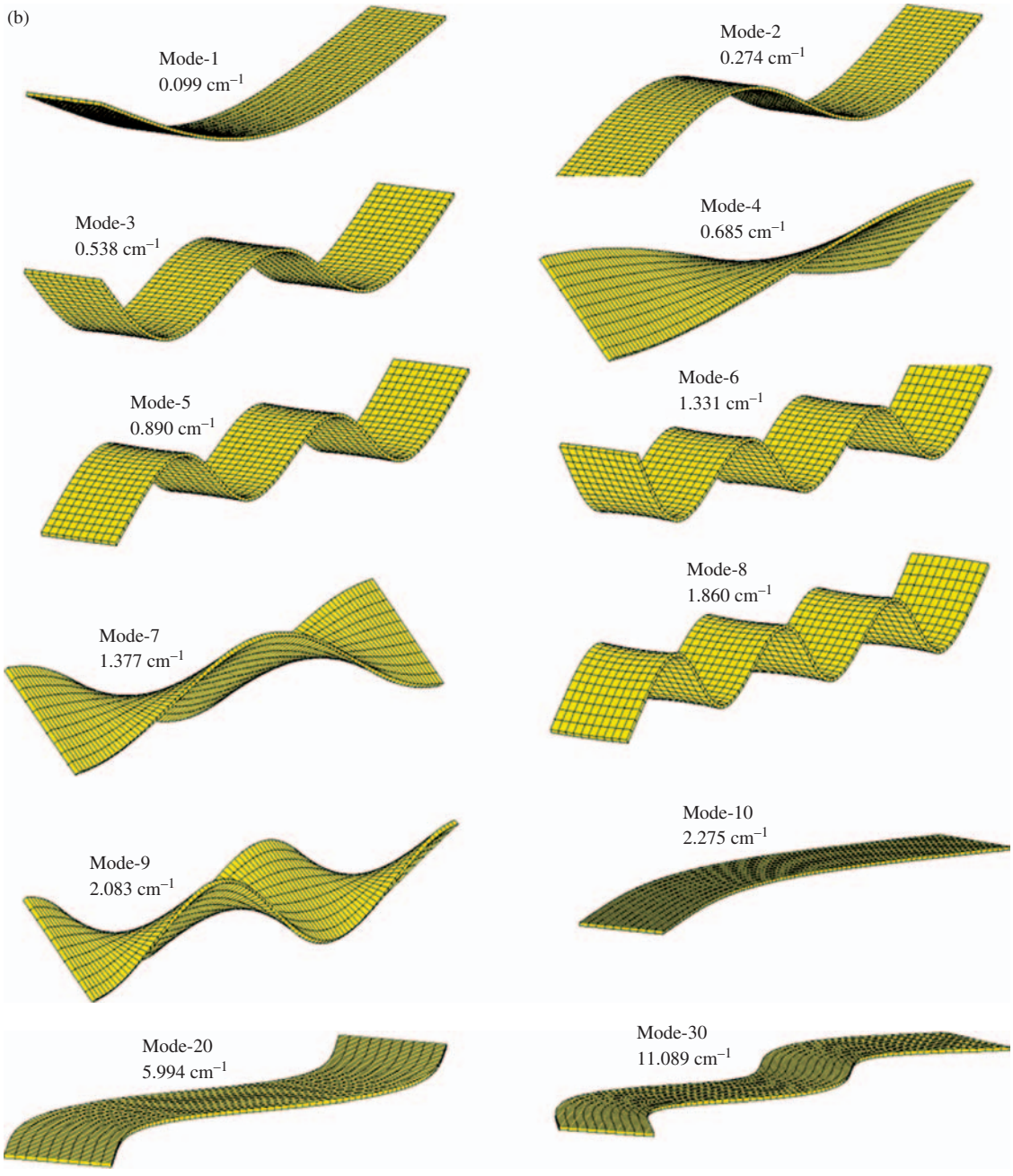

Fig. 9. (a) Modes of free–free 23.53 Å × 262.24 Å armchair graphene strip computed from MM. For modes 1, 2 and 15 bending deformations occur in the plane of the strip. (b) Modes of ECS of free–free 23.53 Å × 262.24 Å armchair graphene strip computed from the 3D-LET. For modes 10, 20 and 30 bending deformations occur in the plane of the ECS similar to modes 1, 2 and 15 shown in Figure 9(a).

where r and s are number of half waves along the x- and the y- directions, respectively, the frequency parameter λ_{rs} depends on the aspect ratio, Poison's ratio and boundary conditions, and γ is the areal mass density (mass/area) of the plate. For clamped and square plates with Poisson's ratio = 0.21, λ_{11}^2, $\lambda_{12}^2 = \lambda_{21}^2$, λ_{22}^2, $\lambda_{13}^2 = \lambda_{31}^2$ equal 35.99, 73.41, 108.3 and 131.6, respectively.[34] Equating the frequency in Eq. (4) for a particular (r, s) mode to that derived from the MM simulations for the SLGS, taking $Eh = 340$ N/m, Poisson's ratio $\nu = 0.21$, areal mass density = (mass of carbon atoms in the SLGS)/(ab), we find the thickness of the ECS or equivalently of the SLGS. These values of h, listed in Table III, equal ∼1 Å. Therefore the bending stiffness, D,of a SLGS equals 1.86 eV. Values of D for graphene sheets reported in the literature vary from 0.69 to 1.5 eV. Arroyo and Belytschko[10] have used the first and the second generation Brenner potentials and found D equal to 0.85 and 0.69 eV, respectively. We note that the Brenner potential does not account for the dihedral torsion term. Lu et al.[22] have shown that the

consideration of the dihedral torsion term in the second generation Brenner potential increases the value of D, and found it to equal 1.4 eV which is close to the 1.5 eV computed by Kudin et al.[9] using an *ab initio* method. The larger value of D in the present computations may be attributed to the consideration of cross interactions among various degrees of freedom in the MM3 potential given by Eq. (1) that are not considered in the Brenner potential.

In order to verify values of elastic constants ($E = 3.4$ TPa, $\nu = 0.21$) and the thickness ($h = 1$ Å) of a SLGS, we compute frequencies and mode shapes of free–free ECS of the 23.53 Å × 262.24 Å armchair SLGS using the commercial finite element (FE) software ANSYS.[36] We use 4-node Shell-63 FE with the membrane and the bending deformations, mass density = 8561 kg/m^3 computed by dividing the total mass of C-atoms in the SLGS by its volume ($V = a \times b \times h$, Fig. 1). From progressive refinement of the FE mesh, a 100×10 FE mesh (along the length and the width directions, respectively) of uniform elements was found to give converged values of natural frequencies. *As should be clear from values listed in Table IV, the first three frequencies of the axial and the bending modes computed from the MM simulations and the FE method differ at most by ∼3%.*

Figure 8 shows for the first two bending modes, the distribution of strains computed from the mean-value atomistic deformation gradient[33] applied to the MM simulation results, and the analysis of the ECS modeled as a shell. A reasonable agreement in the distribution of strains from the two approaches indicates that frequencies of the ECS of an SLGS can be found by regarding it as a shell. Strains plotted in Figure 8 are scalable since they are computed from eigenvectors of the mass weighted Hessian in the MM simulations, and eigenvectors of the ECS.

6. COMPARISON OF FREQUENCIES OF SLGS COMPUTED FROM MM SIMULATIONS WITH THOSE FROM THE LINEAR ELASTICITY THEORY

We now explore if the vibrational response of the 23.53 Å × 262.24 Å SLGS is similar to that of its ECS made of a homogeneous and isotropic linear elastic material with $E = 3.4$ TPa, $\nu = 0.21$ and mass density $\rho =$ 8561 kg/m^3. The mode shapes and the corresponding frequencies obtained with the MM simulations and using the three-dimensional linear elasticity theory are depicted in Figures 9(a) and (b) respectively. Mode shapes for the lowest 15 frequencies computed with MM simulations are exhibited in Figure 9(a). Mode shapes corresponding to the first 10 lowest frequencies and those for modes 20 and 30 obtained by using the linear elasticity theory using ANSYS[36] are shown in Figure 9(b); other modes are not displayed for the sake of brevity. It is clear that for the three bending modes displayed in Figure 7 the two approaches give essentially the same frequencies. However, MM simulations and the analysis of three-dimensional deformations of the ECS made of a homogeneous linear elastic material have dissimilar mode shapes and unequal frequencies

Table 5. Comparison of frequencies of different modes of stretched SLGS B determined from the three-dimensional linear elasticity theory (3-D LET) and the MM simulations.

Size of the SLGS (No. of C-atoms)	Mode (r, s)	MM simulation (THz) ($\Delta = 0.0$ Å)	MM simulation (THz) ($\Delta = 0.2$ Å)	3D-LET (THz) ($\Delta = 0.2$ Å)
32.33 Å × 31.83 Å (464)	(1,1)	0.259	0.579	0.635
	(1,2)	0.623	1.056	1.065
	(2,2)	1.006	1.437	1.432
	(1,3)	1.222	1.651	1.643

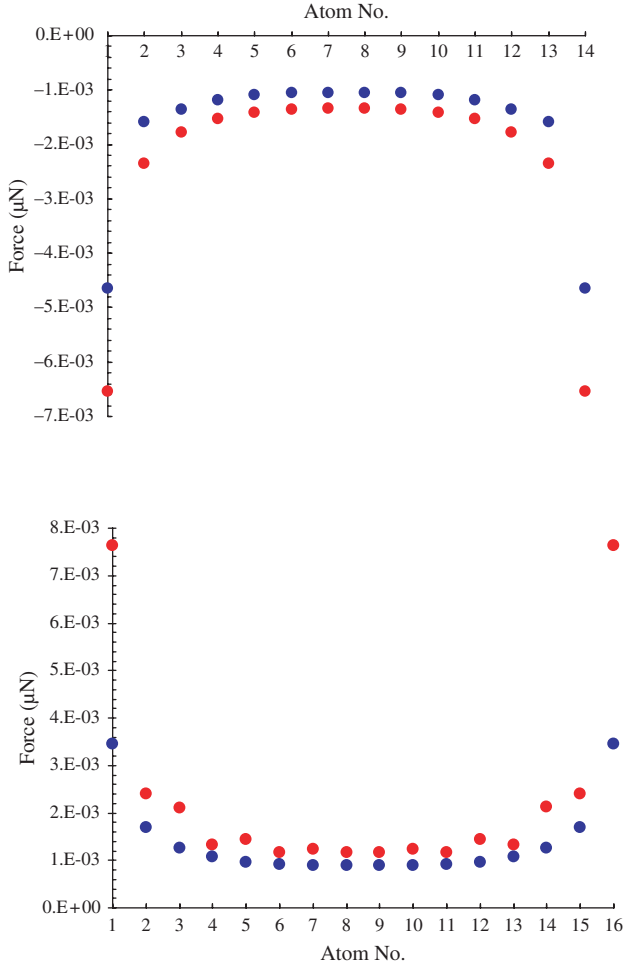

Fig. 10. Distribution of forces on edges (a) 2B and (b) 1R of the 32.33 Å × 31.83 Å graphene sheet and its ECS due to $\Delta = 0.2$ Å. Red filled circles represent magnitude of force computed from the MM simulations and blue filled circles represent magnitude of force computed from the 3D-LET at nodal locations matching with those of atoms in the SLGS.

RESEARCH ARTICLE

implying that a continuum theory cannot predict all mode shapes of a free–free SLGS. It is reported in Ref. [37] that with an increase in the circumferential wave number frequencies of inextensional modes of vibration of (n, 0) zigzag SWCNT saturate at (n-1)/2 or n/2 for odd or even n, but those of the continuum hollow cylinder composed of a linear elastic material do not.

7. FREQUENCIES OF BI-AXIALLY STRETCHED AND CLAMPED SLGS

In experiments of Bunch et al.[28] and Lee et al.[15] graphene sheets had possibly been stretched due to van der Waals interaction of carbon atoms with the silicon atoms of the substrate. This interaction is unavoidable while

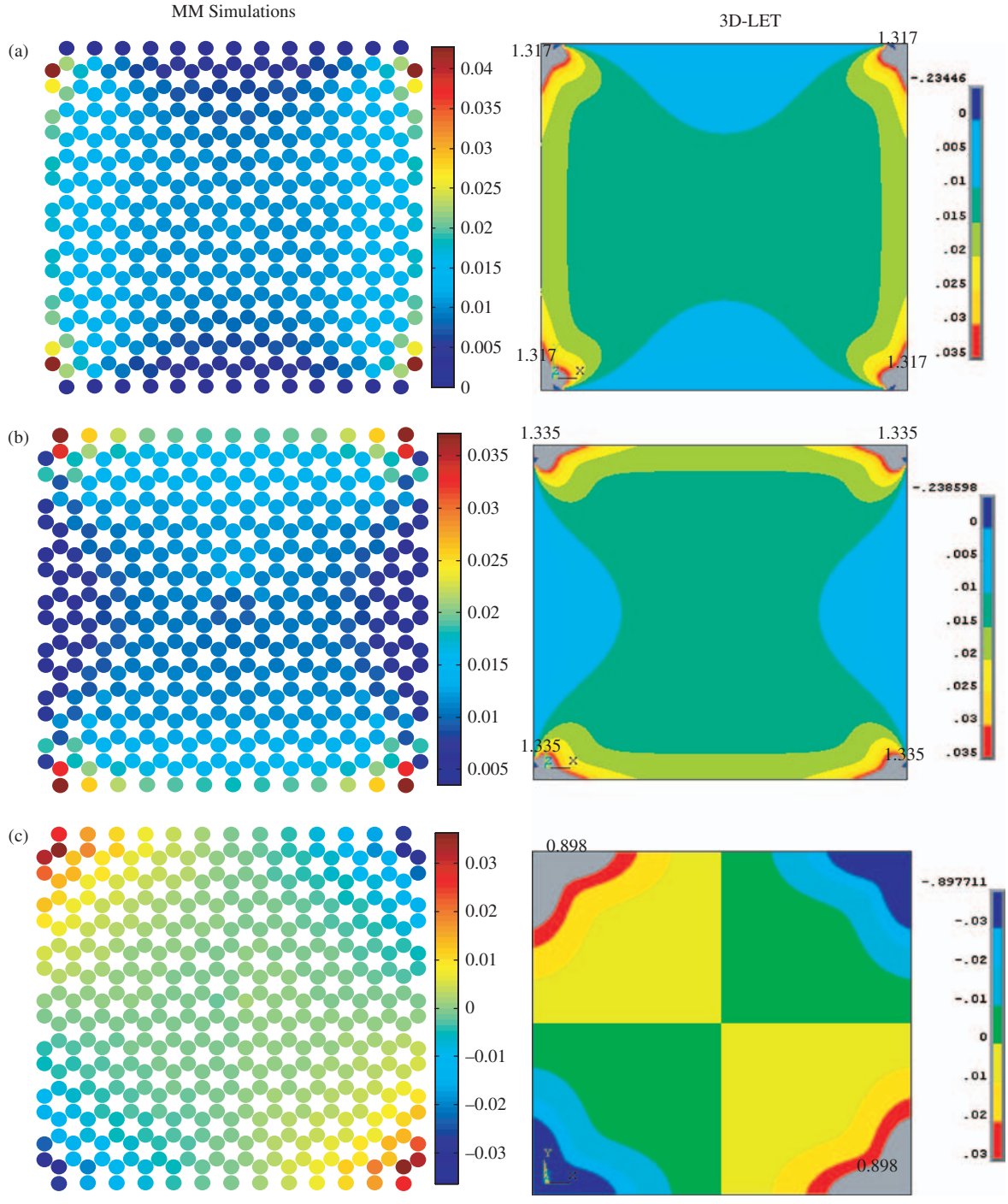

Fig. 11. Distribution of strain components (a) E_{xx}, (b) E_{yy}, and (c) E_{xy} in the 32.33 Å × 31.83 Å graphene sheet and its ECS, for $\Delta = 0.2$ Å prescribed on all edges. Distributions of E_{xx} and E_{yy} are uniform except at points near the edges. The value of E_{xy} is found to be negligible as compared to that of E_{xx} and E_{yy} except at the corners. The values of gray contours in strain distribution plots of the ECS are printed on the contours.

RESEARCH ARTICLE

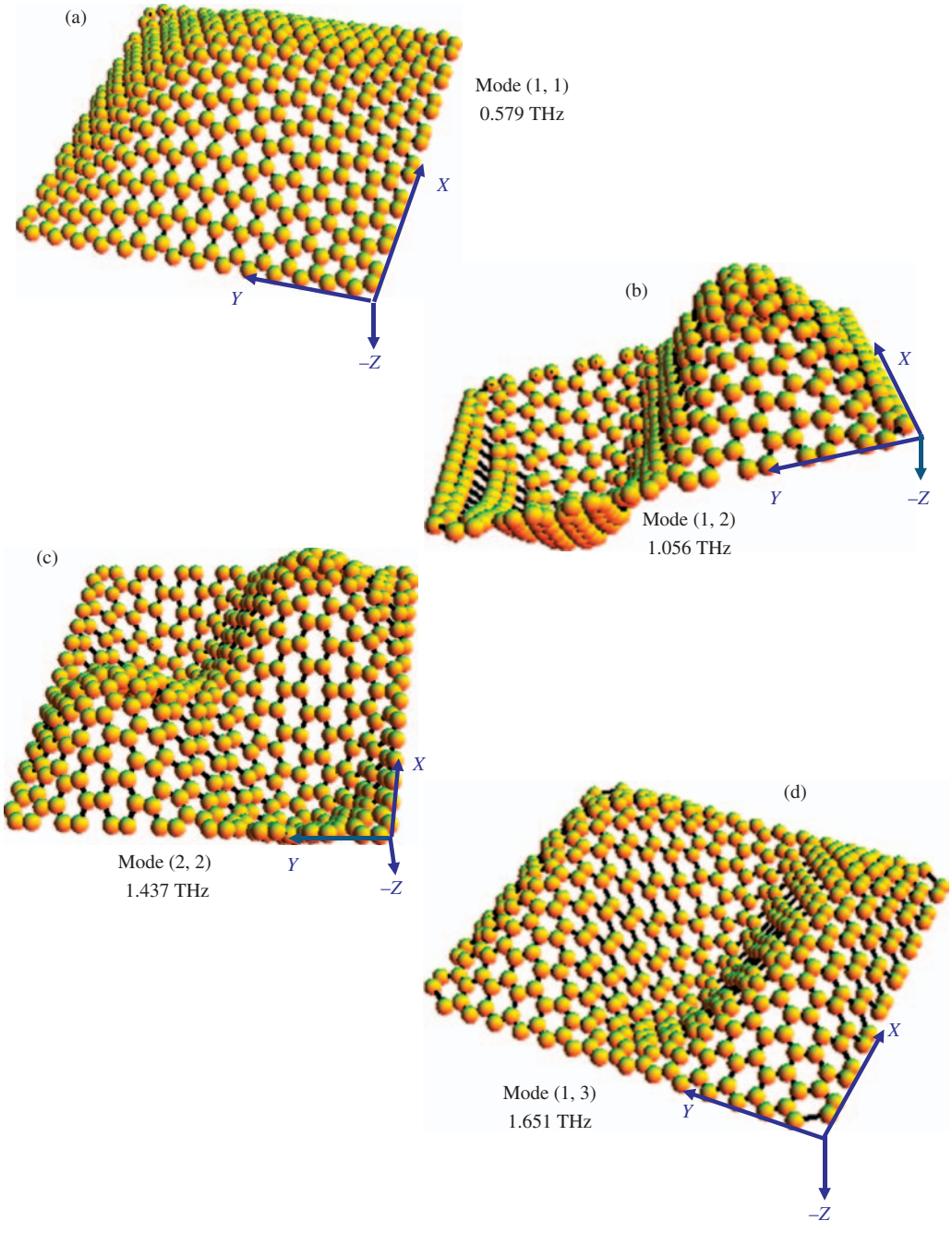

Fig. 12. Mode shapes of the clamped 32.33 Å × 31.83 Å graphene sheet prestretched by ~1.2% in the *x*—and the *y*-directions.

making devices like nanomechanical resonators. Furthermore, some applications (THz nanomechanical resonators) may require significant pretension to increase the transverse stiffness of a graphene sheet which will enhance its natural frequencies.

We have investigated the effect on natural frequencies of pretension in sheet B of Table V. The graphene sheet is stretched by prescribing equal and opposite axial displacement Δ to atoms on opposite faces of the sheet. That is, all atoms on edges 1R and 1L are displaced, respectively, in the positive and the negative x-direction by Δ, and all atoms on edges 2T and 2B are displaced in the positive and the negative y-direction by Δ. The minimum potential energy configurations of graphene sheets for incremental values of Δ are found to within rms gradient of 0.001 kcal/mole/Å. Figures 10(a) and (b) exhibit the distribution of in-plane forces, F_y and F_x respectively, acting perpendicular to edges 2B and 1R of sheet B for $\Delta =$ 0.2 Å. Three-dimensional deformations of the ECS under the same boundary conditions as applied to the SLGS are analyzed with ANSYS[36] using 20-node solid elements to accurately capture the singularity in strains at corners.

The distributions of reaction forces computed at nodes on edges 2B and 1R and having the same spatial locations as atoms in the SLGS are shown in Figure 10. It is found that forces on atoms or nodes at the clamped edge from the two approaches differ by ∼10% for atoms near the middle of the edge, and the differences between the two sets of results are large for atoms at the corners. Furthermore, the distribution of forces at points near the middle of the edges is uniform, while their magnitudes increase for corner atoms. Also we note that the total force acting on atoms on edges 2B and 1R is approximately the same. Figure 11 shows distribution of strains E_{xx}, E_{yy} and E_{xy} in the stretched sheet computed from the mean-value deformation gradient[33] and for its ECS obtained with the FEM; the two sets of results agree with each other qualitatively but distributions near the edges are somewhat different. We find that E_{xx} and E_{yy} are distributed uniformly in the central region of the sheet and $|E_{xy}|$ is negligible as compared to $|E_{xx}|$ and $|E_{yy}|$. Except for the frequency of the fundamental mode, frequencies of (1, 2), (2, 2,) and (1, 3) modes of vibration of the stretched SLGS from the MM simulations and of its linear elastic ECS agree well with each other; these are listed in Table VI. The fundamental mode frequency of the stretched ECS is ∼9.7% more than that of the stretched SLGS; the reasons for this discrepancy are unclear to us. *It is found that for an average axial stretch of ∼ 1.4% in the x- and the y-directions, the fundamental mode frequency of the SLGS and of its ECS has increased by 100% as compared to that of its unstretched state.* The corresponding mode shapes computed from the MM simulations are shown in Figure 12.

8. CONCLUSIONS

The basal plane stiffness of armchair and zigzag single layer graphene sheets (SLGSs) has been determined by studying their uniaxial tensile deformations and free axial and bending mode vibrations with the MM3 potential. The basal plane stiffness is found to be ∼340 N/m which agrees well with that reported in the literature for indentation experiments on graphene sheets. Assuming that the mechanical deformations of a SLGS can be modeled by that of a thin plate having the same dimensions as the SLGS and made of a linear elastic, homogeneous and isotopic material, Poisson's ratio and the wall thickness of the ECS and hence of the SLGS are 0.21 and ∼1 Å, respectively. It is found that the bending vibrations of graphene strips of aspect ratio ∼10 are in their plane which is counterintuitive. Furthermore, mode shapes corresponding to the several lowest frequencies of the free–free SLGS found using the MM simulations differ noticeably from those of the ECS determined by using the linear elasticity theory. The frequencies of vibration of higher modes of a stretched and clamped 1 Å thick plate equal in size to a graphene sheet and made of a linear elastic material computed by using the three-dimensional elasticity theory match well with those of the graphene sheet computed through MM simulations, but the fundamental frequencies from the two approaches differ by 10%. The analysis of free vibrations of a bi-axially stretched clamped square SLGS indicates that an axial stretch of ∼1.2% along the two edges almost doubles the fundamental frequency.

References

1. S. Iijima, *Nature* 354, 56 (**1991**).
2. H. Hiura, T. W. Ebbesen, J. Fujita, K. Tanigaki, and T. Takada, *Nature* 367, 148 (**1994**).
3. H. Roy, C. V. Kallinger, B. Marsen, and K. Sattler, *J. Appl. Phys.* 83, 4695 (**1998**).
4. X. Lu, M. F. Yu, H. Huang, and R. S. Ruoff, *Nanotech.* 10, 269 (**1999**).
5. K. S. Novoselov, D. Jiang, F. Schedin, T. J. Booth, V. V. Khotkevich, S. V. Morozov, and A. K. Geim, *Proc. Natl. Acad. Sci. USA* 102, 10451 (**2005**).
6. S. Stankovich, D. A. Dikin, G. H. B. Dommett, K. M. Kohlhaas, E. J. Zimney, E. A. Stach, R. D. Piner, S. T. Nguyen, and R. S. Ruoff, *Nature* 442, 282 (**2006**).
7. J. F. Nye, Physical Properties of Crystals, Oxford University Press, New York (**1985**).
8. G. Van Lier, C. Van Alsenoy, V. Van Doren, and P. Geerlings, *Chem. Phys. Lett.* 326, 181 (**2000**).
9. K. N. Kudin and G. E. Scuseria, *Phys. Rev. B* 64, 235406 (**2001**).
10. M. Arroyo and T. Belytschko, *Phys. Rev. B* 69, 115415 (**2004**).
11. Y. Huang, J. Wu, and K. C. Hwang, *Phys. Rev. B* 74, 245413 (**2006**).
12. C. D. Reddy, S. Rajendran, and K. M. Liew, *Nanotechnology* 17, 864 (**2006**).
13. E. Konstantinova, S. O. Dantas, and P. M. V. B. Barone, *Phys. Rev. B* 74, 035417 (**2006**).
14. F. Liu, P. Ming, and J. Li, *Phys. Rev. B* 76, 064120 (**2007**).
15. C. Lee, X. Wei, W. Kysar, and J. Hone, *Science* 321, 385 (**2008**).
16. K. H. Michel and B. Verberck, *Phys. Rev. B* 78, 085424, (**2008**).
17. J. Zhou and R. Huang, *J. Mech. Phys. Sol.* 56, 1609 (**2008**).
18. R. Faccio, P. A. Dennis, H. Pardo, C. Goyenola, and Á. W. Mombrú, *J. Phys.: Condens. Matter* 21, 285304 (**2009**).
19. A. Sakhaee-Pour, *Solid State Communications* 149, 91 (**2009**).
20. H. Bu et al., *Phys. Lett. A* (**2009**).
21. F. Scarpa, S. Adhikari, and A. S. Phani, *Nanotech.* 20, 065709 (**2009**).
22. Q. Lu, M. Arroyo, and R. Huang, *J. Phys. D: Appl. Phys.* 42, 102002 (**2009**).
23. M. Klintenberg, S. Lebegue, C. Ortiz, B. Sanyal, J. Fransson, and O. Eriksson, *J. Phys.: Condens. Matter* 21, 335502 (**2009**).
24. E. Cadelano, P. L. Palla, S. G., and L. Colombo, *Phys. Rev. Lett.* 102, 235502 (**2009**).
25. K. Behfar and R. Naghdabadi, *Tech.* 65, 1159 (**2005**).
26. X. Q. He, S. Kitipornchai, and K. M. Liew, *Nanotech.* 16, 2086 (**2005**).
27. K. M. Liew, X. Q. He and S. Kitipornchai, *Acta Materialia* 54, 4229 (**2006**).
28. J. S. Bunch, A. M. van der Zande, S. S. Verbridge, I. W. Frank, D. M. Tanenbaum, J. M. Parpia, H. G. Craighead, and P. L. McEuen, *Science* 315, 490 (**2007**).
29. N. L. Allinger, Y. H. Yuh, and J.-H. Lii, *J. Am. Chem. Soc.* 111, 8511 (**1989**).
30. S. S. Gupta and R. C. Batra, *Computational Materials Science* 43, 715 (**2008**).
31. S. Yu, S. Yang, and M. Cho, *Polymer* 50, 945 (**2009**).

32. J. W. Ponder, User's Guide TINKER MOLECULAR MODELLING PACKAGE 4.2. **(2004)**.
33. J. A. Zimmerman, D. J. Bammann, and H. Gao, *J. Mech. Phys. Sol.* 46, 238 **(2009)**.
34. R. D. Blevins, Formulas for Natural Frequencies and Mode Shapes, Van Nostrand Reinhold Company, New York **(1979)**.
35. User's Manual MATLAB R 2007 A, The MathWorks, Inc., Natick, MA, USA.
36. User's Manual ANSYS 11.0, ANSYS, Inc., Canonsburg, PA, USA.
37. S. S. Gupta, F. G. Bosco, and R. C. Batra, *J. Appl. Phys.* 106, 063527 **(2009)**.

Received: 21 August 2009. Accepted: 30 October 2009.